Helium-3 production from Pb+Pb collisions at SPS energies with the UrQMD model and the traditional coalescence afterburner

Qingfeng Li [1a], Yongjia Wang [1], Xiaobao Wang [1], and Caiwan Shen [1],

1) School of Science, Huzhou University,

Huzhou 313000, P.R. China

arXiv:1603.09084v1 [nucl-th] 30 Mar 2016

(Dated: March 31, 2016)

Abstract

A potential version of the UrQMD (UrQMD/M) transport model and a traditional coalescence model are combined to calculate the production of ^{3}He fragments in central Pb+Pb collisions at SPS energies 20-80 GeV/nucleon. It is found that the Lorentz transformation in the afterburner influences visibly the ^{3}He yield and should be considered in calculations. The rapidity distribution of ^{3}He multiplicities (including the concave shape) can be described well with UrQMD/M when it stops during t_{cut}=100±25 fm/c and the coalescence afterburner with one parameter set of (R_0,P_0)=(3.8 fm, 0.3 GeV/c) is taken into use afterwards.

PACS numbers: 24.10.Lx, 25.75.Dw, 25.75.-q, 24.10.-i

[a] E-mail address: liqf@hutc.zj.cn

I. MOTIVATION AND MODEL SETTINGS

The production and decay properties of nuclei are fundamental many-body problems in the evolution of the universe, which can be studied in artificial laboratories with heavy ion collisions (HICs). Besides the HICs at low and intermediate energies for the synthesis of (super-)heavy nuclei or the multi-fragmentation through a possible liquid gas phase transition, the production mechanism of nuclei in ultra-relativistic HICs deserves more investigation since it may give important message on the quantum chromodynamics (QCD) phase transition from quark-gluon plasma (QGP) to hadron gas (HG) [1]. In addition, if nuclei are formed through a coalescence process one can use their yield ratios to measure the volume of the particle source from which they emerge. This offers important information on the space-time evolution of the reaction, and implies a close relation of space-time structure between the coalescence and the the so-called "femtoscopy" or "HBT" (in reference to Hanbury-Brown and Twisss original work with photons) correlation [2].

In past two decades, profited from some experimental measurements e.g., [2–6], the light fragment production mechanism has being investigated more deeply but mainly with a coalescence afterburner in which a Wigner-function method is in use (called Wigner-coalescence) [7–9]. However, it has the substantial disadvantage of not conserving baryon number in the projection. Therefore, we employ the traditional phase-space coalescence approach frequently used for HICs at low and intermediate energies [10–12] and in this paper as well. In Ref. [13], the method has been used for describing rapidity distributions of both the E895 proton data at AGS energies and the NA49 net proton data at SPS energies with the help of the Ultra-relativistic Quantum Molecular Dynamics (UrQMD) model supplemented by potentials for both pre-formed hadrons and confined baryons (called UrQMD/M) [14, 15], taking the similar density-dependent (Skyrme-like) terms. It is found that, using only one parameter set of (R_0, P_0)=(3.8 fm, 0.3 GeV/c) in the afterburener (where R_0 and P_0 are parameters of relative distance and relative momentum between two particles for constructing clusters), both sets of experimental data can be described reasonably well. This success encourages us to examine further the production yields of light fragments from HICs at high energies. It is noticed that some experimental data related to the production of light clusters such as deuterons, tritons, and ^{3}He have been available [2, 16, 17]. In this paper, the ^{3}He production from central Pb+Pb reactions at SPS energies 20-80 GeV/nucleon is taken as

an example.

The UrQMD microscopic transport model was originally developed to study particle production at high energies such as AGS, SPS, and RHIC energies [18–20]. Recently, it has been updated for simulating HICs at both lower, such as SIS energies [12, 21–24] and higher, such as LHC energies [25–27]. It is interesting to see that the potentials always play an important role on the particle emission from HICs at whatever low or high energies. Especially, with the consideration of mean-field potentials for pre-formed hadrons, some quantities such as the HBT of two particles (especially the time-related HBT-puzzle), the elliptic flow (in the cascade mode calculations, it is known as a flow-puzzle), and the yields of strange baryons or anti-baryons (a puzzle related to the strangeness enhancement) can be better described or explained [14, 15, 28]. Although a thorough explanation of all existing puzzles is still awaiting since a complete description of the multi-particle collision dynamics crossing a possible phase transition and/or a consistency with the first-principle lattice QCD calculations has not arrived yet, the current version of UrQMD (UrQMD/M) is nice for the investigation of the light fragment production mechanism if a suitable afterburner is linked when the UrQMD stops at a certain time t_{cut}.

In the afterburner, as stated in Ref. [13] for protons, the relativistic effect ought to be examined when calculating relative distance δr and relative momentum δp between two baryons. It was found that, due to the large cancellation between the coordinate-spatial expansion and the momentum-spatial shrinkage by the Lorentz transformation (LT) in the afterburner, the proton yield with LT is close to that without LT, although some minor difference between them is still observed. It is interesting to see how the minor difference in proton yield influences the yield of light fragment such as ^{3}He. Fig. 1 depicts the rapidity y ($= \frac{1}{2}\log(\frac{E_{\rm cm}+p_{//}}{E_{\rm cm}-p_{//}})$, where $E_{\rm cm}$ and $p_{//}$ are the energy and longitudinal momentum of the observed particle in the center-of-mass system, respectively) distribution of ^{3}He from central ($< 5\%$ of the total cross section σ_T) Pb+Pb collisions with beam energies $E_b = 20$ and 80 GeV/nucleon. t_{cut}=100 fm/c is chosen. For each beam energy, results with and without consideration of LT are shown for comparison. It is clear that the influence of LT is larger for light fragments than for free nucleons, which is mainly due to their much smaller yields. In addition, the consideration of LT in the afterburner drives further down the yield of ^{3}He, which is attributed to the larger relativistic effect for the momentum difference δp than for the distance difference δr, as discussed in Ref. [13]. Hence, in the following discussions, the

LT effect is always taken into account in the coalescence model.

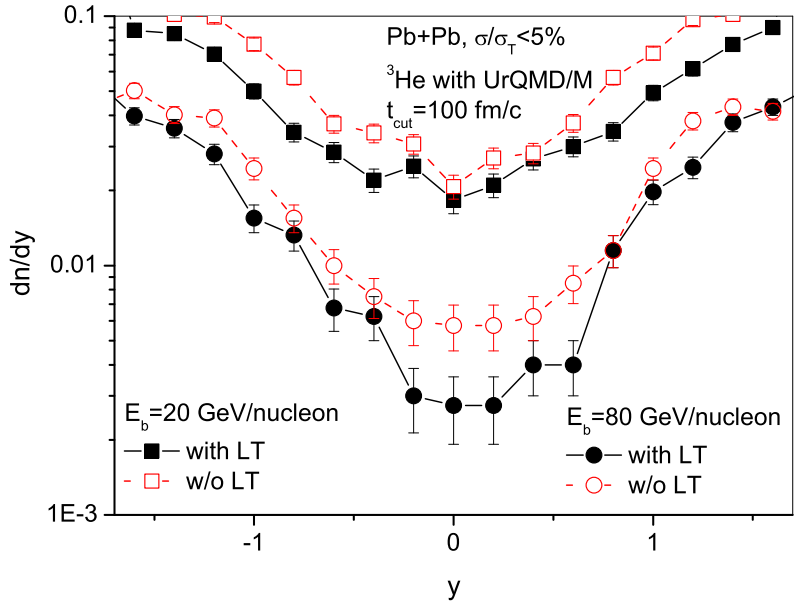

FIG. 1. (Color online) Rapidity distribution of ^{3}He from central Pb+Pb collisions with beam energies E_b = 20 (lines with squares) and 80 GeV/nucleon (lines with circles). t_{cut}=100 fm/c is chosen. For each beam energy, results with (solid symbols) and without (open symbols) LT are shown.

II. TIME DEPENDENCE OF ^{3}HE MULTIPLICITIES

For a systematic survey, the same parameter set (R_0, P_0)=(3.8 fm, 0.3 GeV/c) in the phase-space coalescence model used for protons is still adopted for the current calculations. But, the t_{cut} dependence of the ^{3}He multiplicity should be addressed since it might partly produced later than protons due to the sequential decay of highly-excited heavier fragments. In Fig. 2 we demonstrate the rapidity distribution of ^{3}He multiplicities at two beam energy points 20 (top plot) and 80 GeV/nucleon (bottom plot) and at several stopping times 25, 50, 75, 100, and 125 fm/c (different lines), respectively. Correspondingly, the NA49 experimental data are taken from Ref. [16] (scattered stars). At t_{cut}=25 fm/c, which is known that the high-density compression phase has disappeared for a long time [28], a large amount of nucleons and light fragments are frozen out due to the following low-density environment,

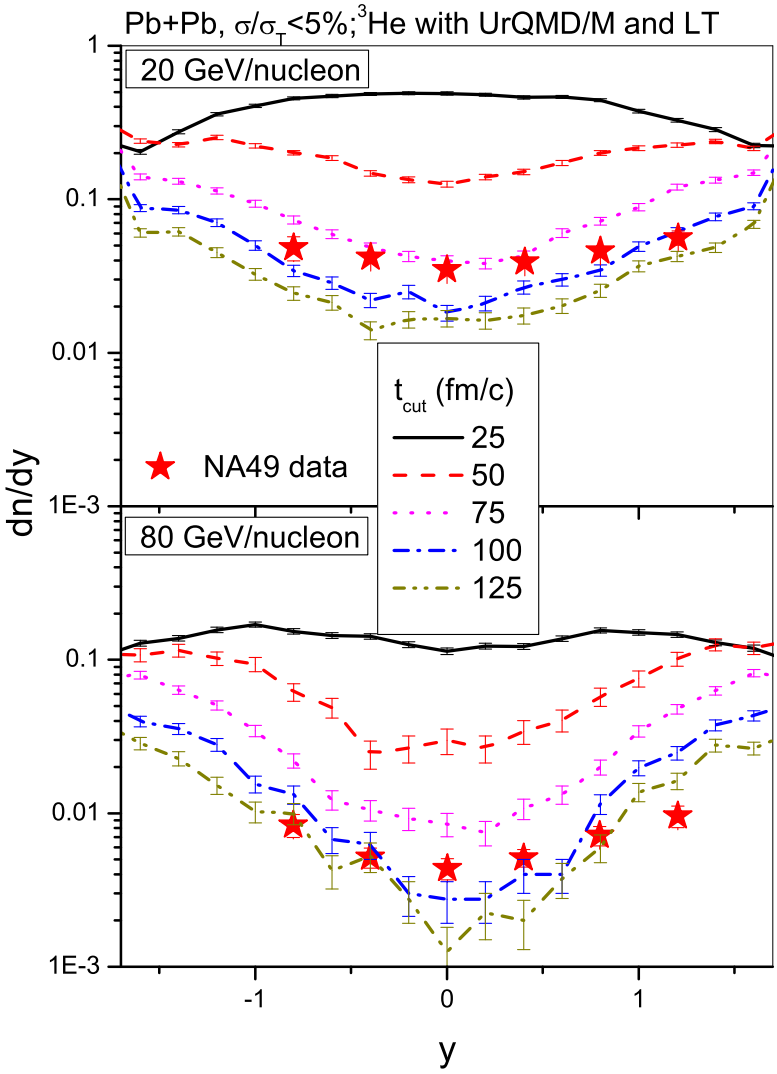

FIG. 2. (Color online) Rapidity distribution of ^{3}He multiplicities at two beam energy points: 20 (top plot) and 80 GeV/nucleon (bottom plot). In each plot, results at t_{cut}=25 (solid line), 50 (dashed line), 75 (dotted line), 100 (dash-dotted line), and 125 fm/c (dash-dot-dotted line) are compared to the NA49 experimental data taken from Ref. [16].

which is seen with the solid lines at both beam energies. However, it is clear that at this time the multiplicities of ^{3}He are at least one order of magnitude larger than experimental data. In addition, the concave shape shown in data can not be described by calculations. It implies that most of the ^{3}He "constructed" at the early times will decay to lighter clusters

such as deuterons and nucleons. With the time increasing from 25 to 75 fm/c, it is seen clearly that the ^{3}He multiplicities are reduced quickly and approach to the data. Meanwhile, the concave shape emerges. Due to larger stopping and more energy deposition, more excited ^{3}He fragments at mid-rapidity decay than those at projectile-target rapidities. As the time increases further, the ^{3}He multiplicities is seen to reduce continuously but with much lower speed. Due to the lack of a statistic treatment for the very late stage, the NA49 data are described well enough within the stopping time t_{cut}=100±25 fm/c for UrQMD/M together with the phase-space coalescence model using the parameter set (R_0, P_0)=(3.8 fm, 0.3 GeV/c). One also finds that it takes longer time for ^{3}He fragments lying away from mid-rapidity to meet the data which is due to the fact that much more heavier fragments exist in these areas and decay to lighter ones such as ^{3}He.

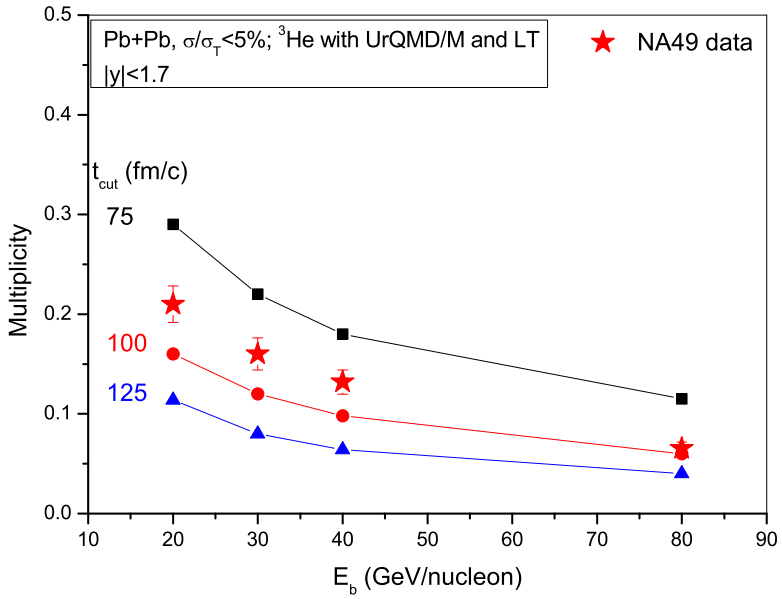

FIG. 3. (Color online) Rapidity-integrated ($|y| < 1.7$) multiplicities of ^{3}He fragments as a function of beam energy, calculated with stopping times 75(line with squares), 100 (line with circles), and 125 fm/c (line with up-triangles) for UrQMD/M. The NA49 data are taken from Ref. [16].

This time dependence can also been seen from the rapidity-integrated ($|y| < 1.7$) multiplicity of ^{3}He fragments which is shown in Fig. 3, as a function of SPS beam energies. Calculations with t_{cut}=75, 100, and 125 fm/c (lines with different symbols) are shown for

comparison to the NA49 data [16] (scattered stars). With the increase of beam energy, the calculated ^{3}He yield decreases and follows data reasonable well. Further, it is interesting to see that it requires a longer time to reach the experimental data of light fragments at higher beam energies. At first glance, it is hard to understand since higher excitation should lead to earlier emission. It is true if we take a look at the decrease of absolute values at one fixed time with beam energies increasing from 20 to 80 GeV/nucleon, as seen in Fig. 2. However, meanwhile, the higher energy of heavier fragments leads to the more sequential decay to lighter fragments which will certainly take a longer time. Therefore, the competition between production and decay of excited ^{3}He fragments at different rapidities determines the quantity and time scale of its final production, during which a proper dynamic treatment is obviously important since it determines the phase-space evolution and the final stability of a fragment. Meanwhile, the production of clusters other than ^{3}He should be also investigated in a systematic manner so that a more complete prospect could be established, which is in progress.

III. SUMMARY

In summary, with a potential version of the UrQMD (UrQMD/M) transport model, and a traditional coalescence model in which one parameter set of (R_0,P_0)=(3.8 fm, 0.3 GeV/c) is used, both the rapidity distribution and the rapidity-integrated multiplicity of ^{3}He fragments in central Pb+Pb collisions at SPS energies 20-80 GeV/nucleon are calculated at several stopping times of the transport program, and with or without considering the Lorentz transformation in the afterburner. It is found that the Lorentz transformation influences visibly the ^{3}He yield and should be considered in the analysis. The rapidity distribution of ^{3}He multiplicities (including the concave shape) can be described well with UrQMD/M when it stops during t_{cut}=100$\pm$25 fm/c and the coalescence afterburner is linked together. The finding that the ^{3}He cluster can only escape at the later freeze-out stage within a dilute environment supports the production mechanism of light fragment via coalescence as well. The universal competition between sequential production and decay of light fragments asks us to consider more carefully both the stiffness of the dynamic evolution and the statistical sequential decay.

ACKNOWLEDGMENTS

We thank Prof. M. Bleicher for valuable suggestions and acknowledge support by the computing server C3S2 in Huzhou University. The work is supported in part by the National Natural Science Foundation of China (Nos. 11375062, 11275068, 11505056, and 11505057), the project sponsored by SRF for ROCS, SEM, the Education Bureau of Zhejiang Province (Y201533176) and the Doctoral Scientific Research Foundation (No. 11447109).

[1] R. Arsenescu *et al.* [NA52 Collaboration], New J. Phys. **5**, 150 (2003).

[2] T. Anticic *et al.* [NA49 Collaboration], Phys. Rev. C **69**, 024902 (2004).

[3] S. C. Johnson, UMI-98-22959.

[4] S. Chekanov *et al.* [ZEUS Collaboration], Nucl. Phys. B **786**, 181 (2007) [arXiv:0705.3770 [hep-ex]].

[5] T. Anticic *et al.* [NA49 Collaboration], Phys. Rev. C **85**, 044913 (2012) [arXiv:1111.2588 [nucl-ex]].

[6] P. Newman and M. Wing, Rev. Mod. Phys. **86**, no. 3, 1037 (2014) [arXiv:1308.3368 [hep-ex]].

[7] R. Mattiello, A. Jahns, H. Sorge, H. Stoecker and W. Greiner, Phys. Rev. Lett. **74**, 2180 (1995).

[8] J. L. Nagle, B. S. Kumar, D. Kusnezov, H. Sorge and R. Mattiello, Phys. Rev. C **53**, 367 (1996).

[9] B. Monreal, S. A. Bass, M. Bleicher, S. Esumi, W. Greiner, Q. Li, H. Liu and W. J. Llope *et al.*, Phys. Rev. C **60**, 031901 (1999) [nucl-th/9904080].

[10] H. Kruse, B. V. Jacak, J. J. Molitoris, G. D. Westfall and H. Stoecker, Phys. Rev. C **31**, 1770 (1985).

[11] Q. Li, Z. Li, S. Soff, M. Bleicher and H. Stoecker, Phys. Rev. C **72**, 034613 (2005) [nucl-th/0506030].

[12] Y. Wang, C. Guo, Q. Li, H. Zhang, Z. Li and W. Trautmann, Phys. Rev. C **89**, 034606 (2014) [arXiv:1305.4730 [nucl-th]].

[13] Q. Li, Y. Wang, X. Wang, and C. Shen, Sci. China Phys. Mech. Astron. **??**, ?? (??).

[14] Q. Li, M. Bleicher and H. Stocker, Phys. Lett. B **659**, 525 (2008) [arXiv:0709.1409 [nucl-th]].

[15] Q. Li, M. Bleicher and H. Stocker, Phys. Lett. B **663**, 395 (2008) [arXiv:0802.3618 [nucl-th]].

[16] C. Blume [Na49 Collaboration], J. Phys. G **34**, S951 (2007) [nucl-ex/0701042].

[17] V. I. Kolesnikov [NA49 Collaboration], J. Phys. Conf. Ser. **110**, 032010 (2008) [arXiv:0710.5118 [nucl-ex]].

[18] S. A. Bass *et al.*, [UrQMD-Collaboration], Prog. Part. Nucl. Phys. **41**, 255 (1998).

[19] M. Bleicher *et al.*, [UrQMD-Collaboration], J. Phys. G: Nucl. Part. Phys. **25**, 1859 (1999).

[20] see UrQMD homepage, www.urqmd.org.

[21] Q. Li, C. Shen, C. Guo, Y. Wang, Z. Li, J. Lukasik and W. Trautmann, Phys. Rev. C **83**, 044617 (2011).

[22] C. Guo, Y. Wang, Q. Li, W. Trautmann, L. Liu and L. Wu, Sci. China Phys. Mech. Astron. **55**, 252 (2012).

[23] Y. Wang, C. Guo, Q. Li and H. Zhang, Sci. China Phys. Mech. Astron. **55**, 2407 (2012).

[24] Y. Wang, C. Guo, Q. Li and H. Zhang, Eur. Phys. J. A **51**, 37 (2015) [arXiv:1407.7625 [nucl-th]].

[25] Q. Li, G. Graf and M. Bleicher, Phys. Rev. C **85**, 034908 (2012) [arXiv:1203.4104 [nucl-th]].

[26] G. Graef, Q. Li and M. Bleicher, J. Phys. G **39**, 065101 (2012) [arXiv:1203.4421 [nucl-th]].

[27] G. Graef, M. Bleicher and Q. Li, Phys. Rev. C **85**, 044901 (2012) [arXiv:1203.4071 [nucl-th]].

[28] Q. Li and Z. Li, Mod. Phys. Lett. A **27**, 1250004 (2012) [arXiv:1010.2570 [nucl-th]].